Korean J. Chem. Eng., 39(4), 973-985 (2022)
DOI: 10.1007/s11814-021-0995-x

pISSN: 0256-1115
eISSN: 1975-7220

A Taguchi approach with electron-beam irradiation to optimize the efficiency of removing enrofloxacin from aqueous media

Hong Thi Bich Truong*, Hiep Nghia Bui, Hieu Trung Nguyen***, Thanh-Luu Pham****,*****,**
Duy Ngoc Nguyen****, Yuan-Shing Perng*******, Linh Thi My Lam********,*********,**
Thi-Dieu-Hien Vo********, Van-Truc Nguyen***********, and Ha Manh Bui***********,†**

*Department of Chemistry, Biology and Environment, Pham Van Dong University, Quang Ngai Province 57000, Vietnam
**Department of Environmental Engineering, Dayeh University, Changhua 51591, Taiwan
***Institute of Applied Technology, Thu Dau Mot University, Thu Dau Mot City, Binh Duong Province 75000, Vietnam
****Graduate University of Science and Technology, Vietnam Academy of Science and Technology, Hanoi 10000, Vietnam
*****Institute of Tropical Biology, Ho Chi Minh City 70000, Vietnam
******Research and Development Center for Radiation Technology, Vietnam Atomic Energy Institute,
Ho Chi Minh City 70000, Vietnam
*******Department of Forestry, National Chung Hsing University, Taichung 40227, Taiwan
********Faculty of Education, An Giang University, An Giang Province 90000, Vietnam
*********Vietnam National University Ho Chi Minh City, Ho Chi Minh City 70000, Vietnam
**********Faculty of Environmental and Food Engineering, Nguyen Tat Thanh University,
Ho Chi Minh City 70000, Vietnam
***********Department of Environmental Sciences, Saigon University, Ho Chi Minh City 70000, Vietnam

(*Received 18 August 2021 • Revised 12 October 2021 • Accepted 24 October 2021*)

Abstract−Electron-beam (EB) irradiation was employed to degrade enrofloxacin (ENR) in an aqueous solution. The algal growth inhibition test revealed that ENR exhibited low toxicity against the cyanobacterium *Arthrospira* sp., with an EC_{50}-96 h value of 5.17 mg/L. The Taguchi design also involved finding the best optimum for ENR treatment using EB. Results revealed that the high-efficiency removal of ENR in an aqueous solution was approximately 98.53% under the optimum conditions of an absorbed dose of 5 kGy, a pH of 5.0, and an initial ENR concentration of 10 mg/L and an H_2O_2 concentration of 2 mM. The ERR degradation under a couple of EB irradiation and H_2O_2 followed pseudo-first-order kinetics, with an R^2 of ~0.970. The major degradation pathways of ENR were suggested by density functional theory, natural bond orbital calculations, and liquid chromatography-tandem mass spectrometry (LC/MS/MS) analysis. Life cycle assessment (LCA) was also performed to evaluate the impact of the EB on removing ENR; the industrial process was designed based on laboratory tests aimed with the ReCiPe tool. The obtained results indicated that energy consumption and H_2O_2 affect environmental impacts with order human health, ecology systems, and natural resource. The LCA also proved that EB could be a green and efficient method for eliminating pharmaceutical contaminants in water.

Keywords: Enrofloxacin, Pharmaceutical, Electron Beam, Life Cycle Assessment

INTRODUCTION

Pharmaceuticals in the environment have resulted in various pernicious effects on aquatic ecosystems [1,2]. Fluoroquinolone families are among the most widely used pharmaceuticals to treat or prevent serious bacterial infections. In particular, Enrofloxacin (ENR) is well known due to its high production and worldwide distribution [3]. After first being registered by the Bayer Corporation under the trade name Baytril in 1991, ENR has become one of the most widely prescribed antibiotics. It is classified as one of the pharmaceutical contaminants with emerging concern due to its persistence, bioaccumulation, and possible transfer to living organisms [4]. ENR has been banned in poultry by the US Food and drug administration (FDA) since 2004 due to its potential to cause antibiotic-resistant infections in humans [5]. Recently, ENR has been recorded at approximately 4.24 μg/L in surface water [6,7]. Andrieu et al. [8] indicated approximately 18% of ENR released in aquaculture from treating most important diseases in catfish farming (*Bacillary Necrosis of Pangasius* and *Motile Aeromonad Septicaemia*). Ebert et al. [4] also demonstrated its high toxicity to aquatic species: *Anabaena flos-aquae* (EC_{50}=172 μg/L) and *Lemna minor* (EC_{50}=107 μg/L). To remove this contaminant from the water source, a number of conventional strategies, such as coagulation [9], adsorption [10-13], and biological processes [14], have been utilized. However, these conventional methods may not be sufficient to eradicate ENR from contaminated water, especially on a commercial scale [15]. Hence, an exploration of innovative strategies is needed to eliminate this pollutant. Among the innovative strategies, advanced oxidation pro-

---

[†] To whom correspondence should be addressed.

E-mail: manhhakg@yahooo.com.vn, manhhakg@sgu.edu.vn

cesses (AOPs) have recently drawn significant attention. Over the past five years, various efforts have explored the applicability of the AOPs systems such as photocatalysis [16-18], ozone treatment [19, 20], activated persulfate [21,22], the electro-Fenton process [23], an electron-beam process [24,25] or gamma-ray [26] in removing ENR or pharmaceutical pollutants from contaminated water. Among the aforementioned AOP techniques, electron beam (EB) has been reported as an effective alternative for degrading pharmaceuticals in water [27]. The EB process involves the excitation of an irradiated solution, inducing the generation of highly reactive radicals, mainly hydroxyl radicals ($^{\bullet}$OH), hydrogen radicals ($^{\bullet}$H), hydrated electrons (e^-), and hydrogen peroxide (H_2O_2), which are capable of decomposing the pollutants into carbon dioxide and water. Moreover, this technique does not require additive chemicals and has less sludge formation, which is more advantaged than other AOPs methods [24]. EB has successfully eradicated a myriad of refractory organic pollutants from contaminated wastewater, such as pesticides [25], urban wastewater [28], textile wastewater [29], slaughterhouse wastewater [30,31] and pharmaceuticals [24,27]. Although much EB had been conducted with toxic organic compounds, scarce literature is still available to remove ENR and the degradation mechanism, especially by-products generating using EB technique [24,25].

Some researchers recently published theoretical calculations to describe how AOPs degrade pollutants [32,33]. These investigations used density functional theory (DFT), which is one of the most widely used and effective theoretical calculation approaches for optimizing geometric designs and predicting electronic structures of molecules using natural bond orbital (NBO) computations [33]. Most calculations aim to determine the positive sites or the highest occupied molecular orbital (HOMO) of the organic molecule where formatted $^{\bullet}$OH or the lowest unoccupied molecular orbital (LUMO) release during AOPs could attack.

The charge distribution and energy level of the localized highest occupied orbitals must therefore be taken into account. The relationship between these two parameters and the degradation of organic molecules in the presence of $^{\bullet}$OH has been studied in several reports [32,34]. The active centers on molecules that are preferentially targeted by $^{\bullet}$OH, which often have a high electron density as well as a large partial negative charge, can be determined using this method. Furthermore, a combination of DFT and liquid chromatography-tandem mass spectrometry (LC/MS/MS) was used to analyze the degradation mechanism.

Aside from abatement strategies, experimental design plays a major role in reducing the time and cost of wastewater treatment. Taguchi method, a type of experimental design that based on orthogonal arrays and signal to noise ratio (S/N) qualification [35,36], has succeeded in improving, optimizing, and interpreting the factor effects in many treatment processes from wastewater of textiles [37], pulp and paper mills [38], oily [35], etc. However, the research literature of Taguchi design on the elimination of ENR using the EB method is still insufficient and the involvement of the design could minimize experiments with the best results on EB treatment [35,36].

The key research goals are to determine the elimination of ENR using the EB technique. The experiments were designed based on the L9 Taguchi array with three variables, absorbed dose, initial pH, and H_2O_2 concentration, to reduce ENR. The decomposition mechanism was also evaluated based on DFT calculations, LC/MS/MS analysis, and ENR solution toxicity on cyanobacteria *Arthrospira* sp. In addition, treatment cost and the environmental impact of the EB process are evaluated using life cycle assessment (LCA) based on organic matter decomposition efficiency and energy requirements using the ReCiPe tool.

MATERIALS AND METHODS

1. Synthetic Solutions

Stock (1,000 mg/L) ENR-contaminated solutions were prepared by dissolving 100 mg of standard ENR (Sigma-Aldrich; CAS No. 93106-60-6) in water purified with a Millipore reverse osmosis purification system. A serial of ENR concentration (10, 15, and 20 mg/L) was prepared by diluting the stock solution with deionized water following previous studies [16,18]. Solvents and other chemicals of analytical grade were used. The chemicals and solutions were stored in the dark at 4 °C.

2. Isolation and Culture Microalgae

The cyanobacteria *Arthrospira* sp. (Fig. 1(a)) was isolated from a canal in south Vietnam and used in this study. The inoculum of

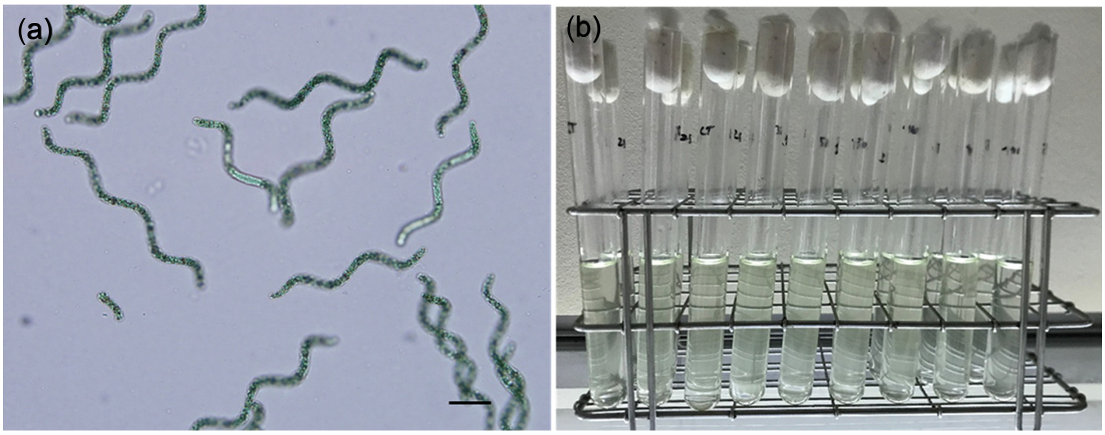

Fig. 1. (a) Microscopic images of *Arthrospira* sp., (b) The algal growth inhibition test. Scale bar: 20 μm.

Arthrospira sp. was cultured in 500-mL Erlenmeyer flasks filled with 300-mL sterilized Z8 medium [39]. All culture was kept at 27± 1 °C, with a photosynthetic photon flux density of 50 μmol photon/m^2/s under a 12 h : 12 h light : dark photoperiod intensity.

3. Algae Growth Inhibition Test

The cells of *Arthrospira* sp. were collected at exponential phase and quantified using a Neubauer counting chamber. The culture was then diluted with a sterilized Z8 medium to achieve the desired density of 5×10^4 cells/mL for further experiments. The algae growth inhibition test was performed according to the OECD 201 guideline methods [40]. Briefly, ENR at the concentrations of 1, 5, 25, 50, 100 mg/L, plus a control (without ENR) was spiked in 25-mL glass tubes filled with 10-mL of Z8 medium and living cells of *Arthrospira* sp. at an initial concentration of 5×10^4 cells/mL (Fig. 1(b)). The test tubes were prepared in triplicate and incubated at the same cultured condition for 96 h. Samples were checked and gently shaken once a day. The density of cells was determined at 24, 48, 72, and 96 h intervals. The median effective concentration (EC_{50}) values that inhibited the 50% growth rate of algae over 96 h (EC_{50}-96 h) were calculated by using the growth rate (GR). The GR of algae for each concentration was determined following Eq. (1):

$$GR=\frac{\ln C_b-\ln C_a}{t_b-t_a} \tag{1}$$

where GR is the growth rate from the time a to time b, C_a is the initial cell density, C_b is the cell density at time b, t_b-t_a is the duration of the test (h). The algal growth inhibition (GI) rate was computed as Eq. (2):

$$\%GI=\frac{GR_C-CR_T}{GR_C}\times 100 \tag{2}$$

where %GI is the percent inhibition; GR_C is the mean growth rate of the control group, and GR_T is the mean growth rate of the treatments.

4. Experimental Design

EB irradiation screening experiments with or without H_2O_2 for different dose (1 to 5 kGy) were performed according to our previous study [24]. Briefly, 1,000 mL of ENR solution at natural pH value (around 5) was put in a plastic box (solution thickness of 2.5 cm), a volume H_2O_2 then was added to the box to reach a dosage of 2 mM; after that, the box was irradiated at specific absorbed doses (0.5 to 5.0 kGy) for 1.5 seconds in an electron accelerator UERL-10-15S2 (10 MeV, 7.5 kW), running on a conveyor (0-24 m/min) at the Research and Development Center for Radiation Technology, Vietnam Atomic Energy Institute, Ho Chi Minh City. Then, the Taguchi experiment was conducted to determine the conditions optimal for the ERN removal via the EB process. Four independent variables were applied: initial pH (X_1), ENR concentration (X_2), H_2O_2 dosage (X_3), and absorbed dose (X_4). The level of each code ranged from low (−1) to high (1), as shown in Table 1 based on our previous screening experiments.

Table 1. Factors and their level used for the design of experiments by the Taguchi method

Independent factors	Level 1	Level 2	Level 3
Initial pH - X_1	5	7	9
ENR concentration - X_2 (mg/L)	10	15	20
H_2O_2 dosage - X_3 (mM)	1	2	3
Absorbed dose - X_4 (kGy)	1	3	5

5. ENR Degradation Kinetics

The ENR decomposition reaction under the action of EB has the following velocity expression (Eq. (3)):

$$v=-\frac{dA}{dt}=[A]^m[B]^n \tag{3}$$

where A, B, m, n are the ENR concentration, the concentration of the oxidizing agent, the reaction order with respect to A, and the reaction order concerning B. However, when EB irradiation is carried out at a constant energy level, the concentration of oxidizing agent B in an aqueous solution over time can be considered constant. So, now the above (m+n) reaction order is reduced to a pseudo-m reaction order. The ENR degradation kinetics were expressed by pseudo-first, pseudo-second, pseudo-third models described in Eqs. (4)-(6) [27,34].

$$\text{Pseudo-first-order reaction:}\quad \ln\frac{A_0}{A}=kt \tag{4}$$

$$\text{Pseudo-second-order reaction:}\quad \frac{1}{A}-\frac{1}{A_0}=kt \tag{5}$$

$$\text{Pseudo-third-order reaction:}\quad \frac{1}{A^2}-\frac{1}{A_0^2}=2kt \tag{6}$$

where A_0 is the concentration of the initial ENR solution, A is the concentration of the ENR solution at time t and k is the rate constant of ENR degradation.

6. Theoretical Calculations

The optimization of the geometry and electronic structure of the ENR molecule and its intermediates was performed by calculations based on density functional theory (DFT) using Gaussian09W with the basis set of 6-311++g(d,p) in the PCM (Polarizable Continuum Model) water solvent model. NBO populations of these substances were performed on the NBO6 software [24,25].

7. Analysis and Statistical Method

Radiochromic film dosimeter [41] was employed to measure absorbed doses during EB irradiation. While ENR residuals were determined using LC-tandem MS equipped with a turbo spray electrospray (ESI) interface (Agilent Technologies, Palo Alto, CA and MS/MS, 4000 QTRAP, Applied Biosystems, USA) with m/z transitions of 360.2→342.2 and 316.2 with the limit of detection (LOD) value at 10 ng/L [42]. The initial solution pH values were determined using an Inolab 740 pH meter. The energy consumption (E_{con}) of EB was computed according to absorbed dose (D) and radiation energy utilization efficiency (f), which are typically 0.5 for UELR-10-15S2 electro accelerator as Eq. (7) follows [25].

$$E_{con}=\frac{D}{3.6\times f} \tag{7}$$

Treatment costs in this study only involve energy consumption and H_2O_2 costs. Given the Vietnamese market in July 2021, the electrical energy price is 0.065 $/kWh and H_2O_2 -30% price 2.0 $/ liter. Therefore treatment costs were calculated by Eq. (8).

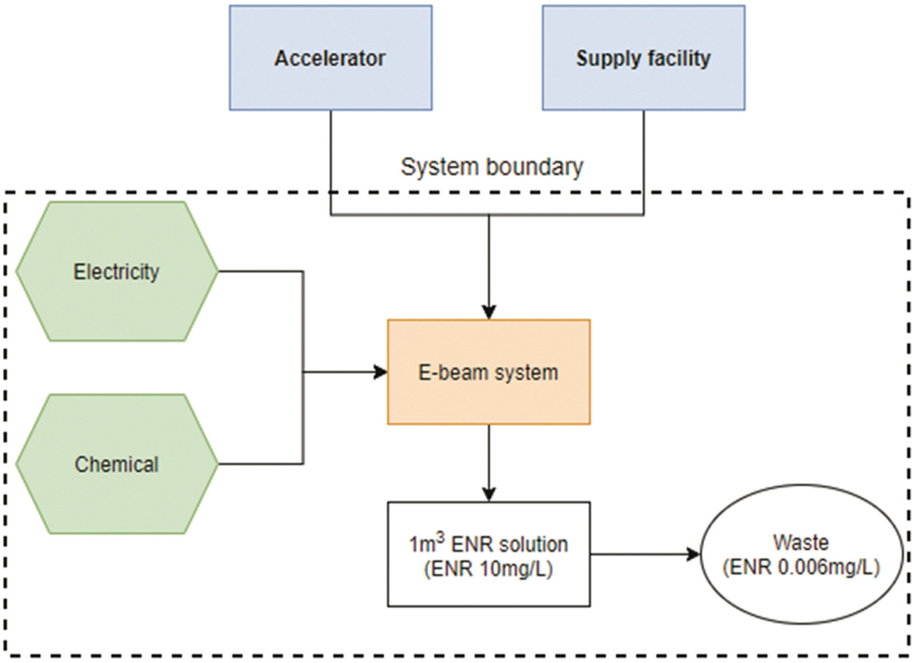

Fig. 2. The system boundary of this work.

$$\text{Treatment cost } (\$/m^3) = 0.0065 \times E_{con} + 2 \times V_{H_2O_2} \tag{8}$$

where $V_{H_2O_2}$ could be determined by Eq. (9).

$$V_{H_2O_2}(\text{liter}) = \frac{10C_{M_{H_2O_2}} \times M_{H_2O_2}}{300D_{H_2O_2}} \tag{9}$$

Here $C_{M_{H_2O_2}}$, $M_{H_2O_2}$ and $D_{H_2O_2}$ are optimal concentration (mM), molecular weight (34.0147 g/mol) and density (1.45 g/mL) of H_2O_2.

The results are displayed as mean±SD. The difference among groups was analyzed by one-way ANOVA, followed by paired t-test, involving Minitab 18.1 version (Minitab Inc, USA); statistically significant differences were considered $p<0.05$.

8. LCA Application

A life cycle assessment (LCA) study was conducted according to the ISO 14040/44 guidelines [43], following an attributional approach. The assumptions and data are detailed in the following sections, starting with the goal and scope, the boundary, the description, and the inventory data and assumptions for the ENR treatment process.

8-1. Goal and Scope

LCA was used to assess the emission impact on the environment and selected metrics of treating 1 m^3 of contaminated ENR using EB. The midpoint and endpoint LCIA metrics analyzed were global warming freshwater ecosystems (GWF), global warming terrestrial ecosystems (GWT), global warming human health (GWH), ozone formation terrestrial ecosystems (OT), ozone formation human health (OH), stratospheric ozone depletion (SOD), Ionizing radiation (ION), fine particulate matter formation (FMF), terrestrial acidification (TA), freshwater eutrophication (FE), marine eutrophication (ME), terrestrial ecotoxicity (TE), freshwater ecotoxicity (FE), marine ecotoxicity (ME), Human carcinogenic toxicity (HCT), human non-carcinogenic toxicity (HNCT), land use (LU), mineral resource scarcity (MRS), fossil resource scarcity (FRS), water consumption Human health (WHH), water consumption terrestrial ecosystem (WTE), and water consumption aquatic ecosystems (WAE). The regulated LCA of the treatment of ENR process using EB focused on determining the life cycle impact assessment (LCIA) indices in EB treatment. Other waste treatment options such as landfill, water reuse are not within the scope of this study and will be addressed in a future study. Finally, the sensitivity of the LCIA metrics to changes in chemicals and energy during the treatment process was evaluated using the ReCiPe method in the SimaPro version 9.2 software [44]. The ReCiPe tool was selected because it can include a set of combined mid-impact and end-effect items to assess sustainability compared to other tools such as CML2002, EcoIndicator 99, Tracy21. The reCiPe can take into account long-term, preventive environmental impacts [45].

8-2. System Boundary

The systemic boundary (Fig. 2) of this study is the elimination of ENR using the EB process. The data used for the life cycle inventory model includes chemical and energy inputs to remove ENR from aqueous solution using EB irradiation. Inputs such as electricity and H_2O_2 reflect regional supplies, Vietnam's electricity grid, and foreign trade in chemicals. The transportation ENR solution from the factory to the laboratory was not calculated and brought inside the boundary. This study was carried out on a laboratory scale and land use was also not taken into account.

8-3. Life-Cycle Inventory (LCI)

The physical relationship during the EB treatment through mass and energy was evaluated using ISO 14040/44 [43]. All chemical mass and energy values are displayed in Table 2. As seen, most chemicals and energy are listed with focusing on the power consumption of EB systems, H_2O_2 and ENR with the functional unit are 1 m^3 of ENR solution at the optimum condition treatment (5 kGy of absorbed dose, 10 mg/L of ENR concentration and 2 mM of

Table 2. Summary of LCI of ENR treatment using EB per functional unit

Items	Values
Energy consumption (kWh)	2.78
H_2O_2 (L)	0.51
ENR (g)	10
Water (m^3)	1
ENR removal (%)	98.53
Treatment time (second)	2.5

H_2O_2 dosage at initial pH 5). With output 6 mg/m^3 of ENR at optimal removal efficiency (99.94%) and all other data could be provided by SimaPro proprietary with Ecoinvent 3 tool.

8-4. Life Cycle Impact Assessment (LCIA)

Life cycle impacts of the ENR removal were assessed using ReCiPe 2016. The impacts associated with the treatment process under study were evaluated in terms of 22 impact categories on the midpoint, i.e., GWF, GWT, GWH, OT, OH, SOD, ION, FMF, TA, FE, ME, TE, FE, ME, HCT, HNCT, LU, MRS, FRS, WHH, WTE and WAE and three impact items on the endpoint, i.e., resource, ecosystems and human health. Some of the data needed in the present study were obtained from previous studies in Simapro relevant to our case study.

RESULTS AND DISCUSSION

1. Algal Growth Inhibition

The inhibition of ENR at the concentration from 1 to 100 mg/L on the cyanobacterium *Arthrospira* sp. after 96 h exposure is shown in Fig. 3. Exposure to ENR at different concentrations resulted in a concentration-dependent inhibition on the growth of *Arthrospira* sp. ENR at the concentration of 50 mg/L or higher inhibited the growth of *Arthrospira* sp. completely. The calculated EC_{50}-96 h value of ENR for *Arthrospira* sp. was 5.17 mg/L.

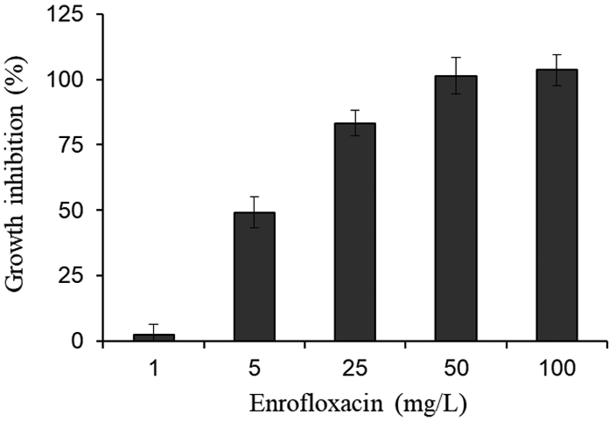

Fig. 3. The growth inhibition of ENR on *Arthrospira* sp. during 96 h of cultivation.

Previous studies have reported the ecotoxicological effects of ENR on microalgae species. Several EC_{50} values were reported for cyanobacteria, green algae, and free-floating aquatic plants, with a wide EC_{50} values variation, ranging from 173 µg/L (EC_{50}-72 h) to 59.16 mg/L (EC_{50}-96 h) [4,46,47]. Cyanobacteria species have been reported to be the most sensitive to ENR [4]. Our results are consistent with previous observations that there was negligible growth inhibition on microalgae species at low ENR concentration (≤1 mg/L), while high concentrations (≥1 mg/L) resulted in significantly inhibited the growth of different microalgae [46,47].

2. Screening Experiments

Results revealed that the highest ENR removal efficiencies of 99.7%, 77.8%, and 6.6% were achieved by EB/H_2O_2, EB, and H_2O_2, respectively (Fig. 4). ENR was rapidly removed by the EB/H_2O_2 and EB treatments but barely eliminated under 1 mM H_2O_2. The ENR removal represented satisfied the pseudo-first-order model, with a removal rate of 0.789 kGy^{-1} for EB/H_2O_2 treatment, and the pseudo-third-order model, with a removal rate of 4.83×10^{-3} L^2/

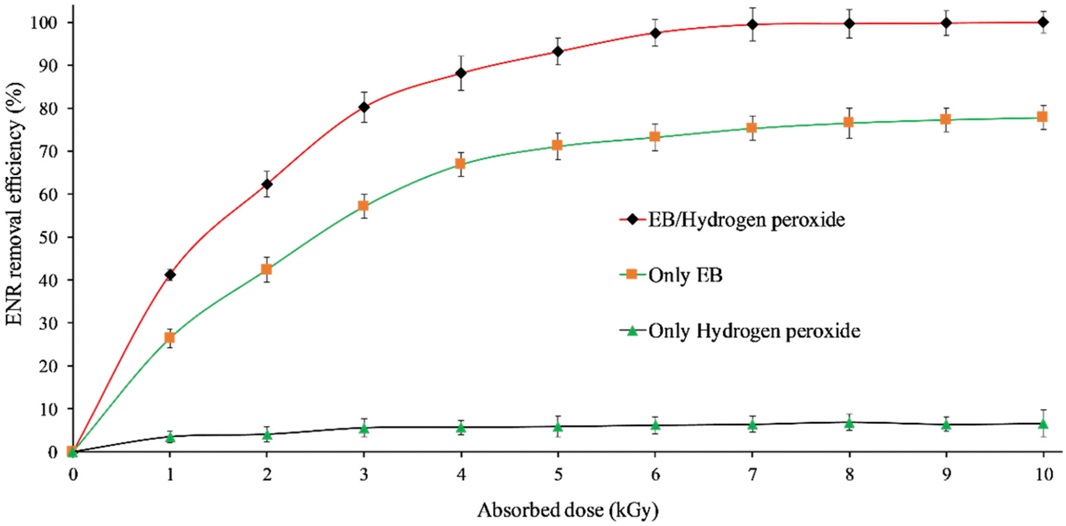

Fig. 4. ENR removal efficiency by EB/ H_2O_2 (1 mM), EB and H_2O_2 (1 mM) at pH 5 and ENR of 15 mg/L.

Table 3. Kinetic model parameters for the ENR removal using EB and H_2O_2

Factors	Reaction order	Regression equation	k	R^2	$^*D_{50}$ (kGy)
EB/H_2O_2	1	**$y=0.789x-0.577$**	**7.89×10^{-1} (1/kGy)**	**0.9702**	**0.879**
	2	$y=12.3x-34.2$	12.3 (L/mg·kGy)	0.3809	5.42×10^{-3}
	3	$y=2309x-6877$	1,154 (L^2/mg^2·kGy)	0.2665	5.77×10^{-6}
EB	1	**$y=0.147x+0.281$**	**1.47×10^{-1} (1/kGy)**	**0.8813**	**4.72**
	2	$y=0.0251x+0.0797$	2.51×10^{-2} (L/mg·kGy)	0.9545	2.66
	3	**$y=9.66\times10^{-3}x+4.58\times10^{-4}$**	**4.83×10^{-3} (L^2/mg^2·kGy)**	**0.9806**	**1.38**

$^*D_{50}$ represents the dose (kGy) required to decompose 50% of the ENR concentration

Table 4. Descriptive statistics and paired sample t-tests for the ENR removal by the EB and H_2O_2

					95% CI for μ difference			
Sample	N	Mean	StDev	SE mean	Lower	Upper	t	p-value
H_2O_2	11	5.21	2.02	0.61	0.00	6.60	-	-
EB	11	58.57	32.07	7.68	0.00	77.81	-	-
EB/H_2O_2	11	78.33	32.07	9.67	0.00	99.97	-	-
*H_2O_2 - EB	22	53.36	23.50	7.09	37.57	69.15	7.53	<0.001
*H_2O_2 - EB/H_2O_2	22	73.12	30.08	9.07	52.91	93.32	8.06	<0.001
*EB -EB/H_2O_2	22	19.76	7.06	2.13	15.02	24.50	9.28	<0.001

*Comparison between groups

Table 5. Experimental and S/N ratio results of the removal ENR using EB

Run	Initial pH	ENR con. (mg/L)	H_2O_2 dosage (mM)	Absorbed dose (kGy)	S/N ratio	ENR removal (%)
1	5	10	1	1	38.8113	87.21
2	5	15	2	3	39.2132	91.34
3	5	20	3	5	39.2861	92.11
4	7	10	2	5	39.8236	97.99
5	7	15	3	1	38.3396	82.60
6	7	20	1	3	38.5073	84.21
7	9	10	3	3	38.9231	88.34
8	9	15	1	5	38.2922	82.15
9	9	20	2	1	37.6437	76.24

mg^2·kGy by only EB treatment (Table 3). These kinetic orders are confirmed in previous studies when the authors use EB to eliminate diclofenac [27] and ofloxacin [34].

The results also suggest that the increment of EB could accelerate the removal of ENR. However, the further EB increase (higher 5 kGy) does not significantly improve removal efficiency. While the combination of H_2O_2 and EB substantially ameliorates the ENR removal efficiency, this significance is also confirmed by a paired t-test between three groups of EB/H_2O_2, EB, and H_2O_2, respectively, with a p-value of ~0.000 (Table 4). The results suggest that the increase in the ENR removal efficiency using H_2O_2 is mainly related to the synergistic effect, which enhanced $^{\bullet}OH$ formation by H_2O_2 in EB irradiation via Eqs. (10) and (11) [24].

$$e^-_{aq}+H_2O_2\rightarrow{}^{\bullet}OH+OH^- \tag{10}$$

$$H^{\bullet}+H_2O_2\rightarrow{}^{\bullet}OH+H_2O \tag{11}$$

Previous studies [24,25] also have reported that some persistent organic compounds in wastewater are successfully removed via a combination of EB and H_2O_2. Based on the results obtained from screening experiments, the two factors, H_2O_2 and absorbed dose, respectively, combined with a concentration of ENR and initial pH, are included in the Taguchi experiment to determine the conditions optimum for ENR removal.

3. Evaluation of Taguchi Approach

The data of the L9 experiment design for EMR removal are presented in Table 5.

The obtained results indicate that the highest removal efficiencies reached 97.99% at experiment number 4 (Absorbed dose 5 kGy, H_2O_2 3 mM, ENR con. 10 mg/L at pH 7), while trial number 9 (Absorbed dose 1 kGy, H_2O_2 2 mM, ENR con. 20 mg/L at pH 9) indicated the lowest yield of 76.24%. The output signal-noise (S/N) ratio from the analysis Taguchi would be estimated to be "the larger,

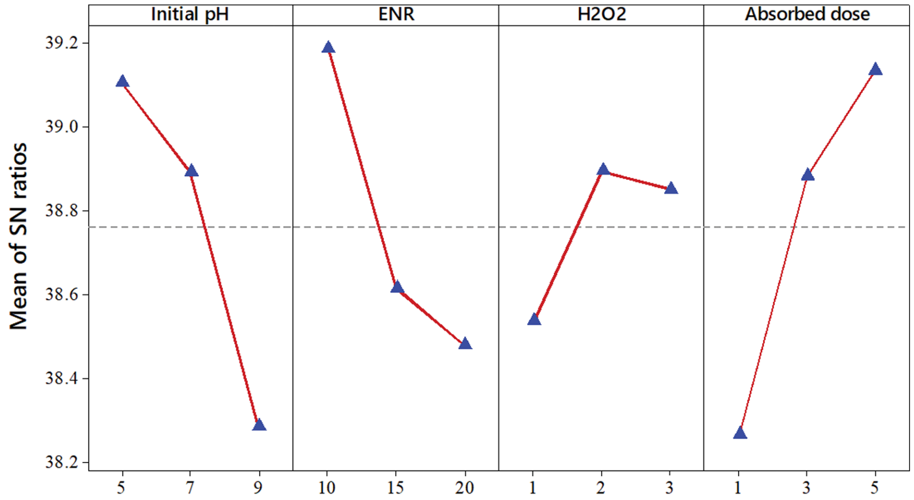

Signal-to-noise: Larger is better

Fig. 5. The main effect of factors on the S/N ratio for ENR removal using EB.

the better" for every test run to identify the distinguishing characteristics between control or signal factors to maximize the ENR removal process. S/N ratio, the ratio of signal power to the noise power, determines the desired signal level to background noise level; the higher the S/N ratio, the higher the molarity of sufficient information than noisy false data. The level and rank of the S/N ratio and mean for each factor are indicated in Tables S1, S2, and Fig. 5.

The S/N ratio implies that the highest efficiency reached in experiment trial 4 may not be optimized. It can be seen that all factors are more critical because they have S/N higher than 37 value, the horizontal S/N value for the influence. The influence of these factors could be decreased following absorbed dose, initial pH, ENR, and H_2O_2 concentration. The response with the highest S/N ratio always performs the optimum results. Therefore, the best combination of factors to obtain the maximum value for S/N ratio and consequently ENR removal efficiency of EB process is absorbed dose level 3 (5 kGy), ENR concentration level 1 (10 mg/L), and H_2O_2 dosage level 2 (2 mM) at initial pH level 1 (5). The predicted combination trials gave a 99.94% theoretical yield with an S/N of 40.04, which was calculated by Minitab software. These experiments were conducted in triplicate and reached the obtained ENR removal around 98.53%. The results align with our previous finding [25] when eliminating most of 4 mg/L of tricylazole at 3.5 kGy absorbed dose and 4 mM H_2O_2.

4. Effect of Absorbed Dose

Absorbed dose plays a critical role in removing ENR during EB irradiation because absorbed dose can navigate the formation of radicals during EB irradiation, especially $^{\bullet}OH$, which could decompose ENR from aqueous solution as following Eq. (12) [25].

$$H_2O \rightsquigarrow 2.8{}^{\bullet}OH+2.7e^{-}_{aq}+0.6H^{\bullet}+0.72H_2O_2+2.7H_3O^{+}+0.48H_2 \qquad (12)$$

As seen in Fig. 5, the S/N ratio of absorbed dose ranks number 1, which varies from 38.26 to 39.13. At first, the increase in absorbed dose from 1 to 3 kGy results in a significant rise in ENR removal yield; however, the removal efficiency slightly increases with a further rise in absorbed dose. These discrepancy results are in line with other previous EB reports [24,25] and can be explained due to the predominant reaction between formed $^{\bullet}OH$ and a by-product as compared with ENR at the first stage, which leads the slight increment in ENR removal efficiency. This trend is also evaluated by the contour plots (Fig. 6(a), (b), and (c)); the best removal ENR reaches at the absorbed doses ranges of 4 to 5 kGy; out of these range values, the absorbed dose has no significant effect on the removal of ENR efficiency.

4-1. Effect of Initial pH

In this series of EB experiments, pH ranks as number 2 the influence factor. As observed in Figs. 6(a), (d), and (e), the initial pH is higher than 7 the ENR removal rate is relatively slow. These results may be explained by the lower redox potential of $^{\bullet}OH$ as pH decreased, as in Eq. (13) [48].

$$E^0=E^0_{HO^{\bullet}/H_2O_2}-0.059\text{pH} \qquad (13)$$

The redox potential of $^{\bullet}OH$ slightly decreased from 2.505 to 2.269 with increased pH 5 to 9. The results correspond to the reduction in S/N ratio from 39.10 to 38.29 as in Fig. 4; another possible explanation for these results could be that with increasing pH value, ENR changed the positive charged to negatively charged forms [12]; the later forms react inefficiently with $^{\bullet}OH$ radical, hence reducing ENR removal efficiency. These reducing trends with the different pH in EB irradiation agree well with previous studies [24,30,31].

4-2. Effect of ENR Concentration

It may very well be contended that the removal efficiency depends on the ENR concentration [12,18,19.21]. As illustrated in Figs. 6(b), (d), and (f), ENR removal efficiency decreases with increasing ENR concentration. The removal efficiency was sharply reduced to 96% at ENR concentration below 12 mg/L, a further rise in ENR concentration, leading the removal results to sharply decrease. This substantial reduction was possibly related to fixed $^{\bullet}OH$ formation that could inadequately react to the increasing ENR. Besides, at increasing ENR initial concentration, the number of

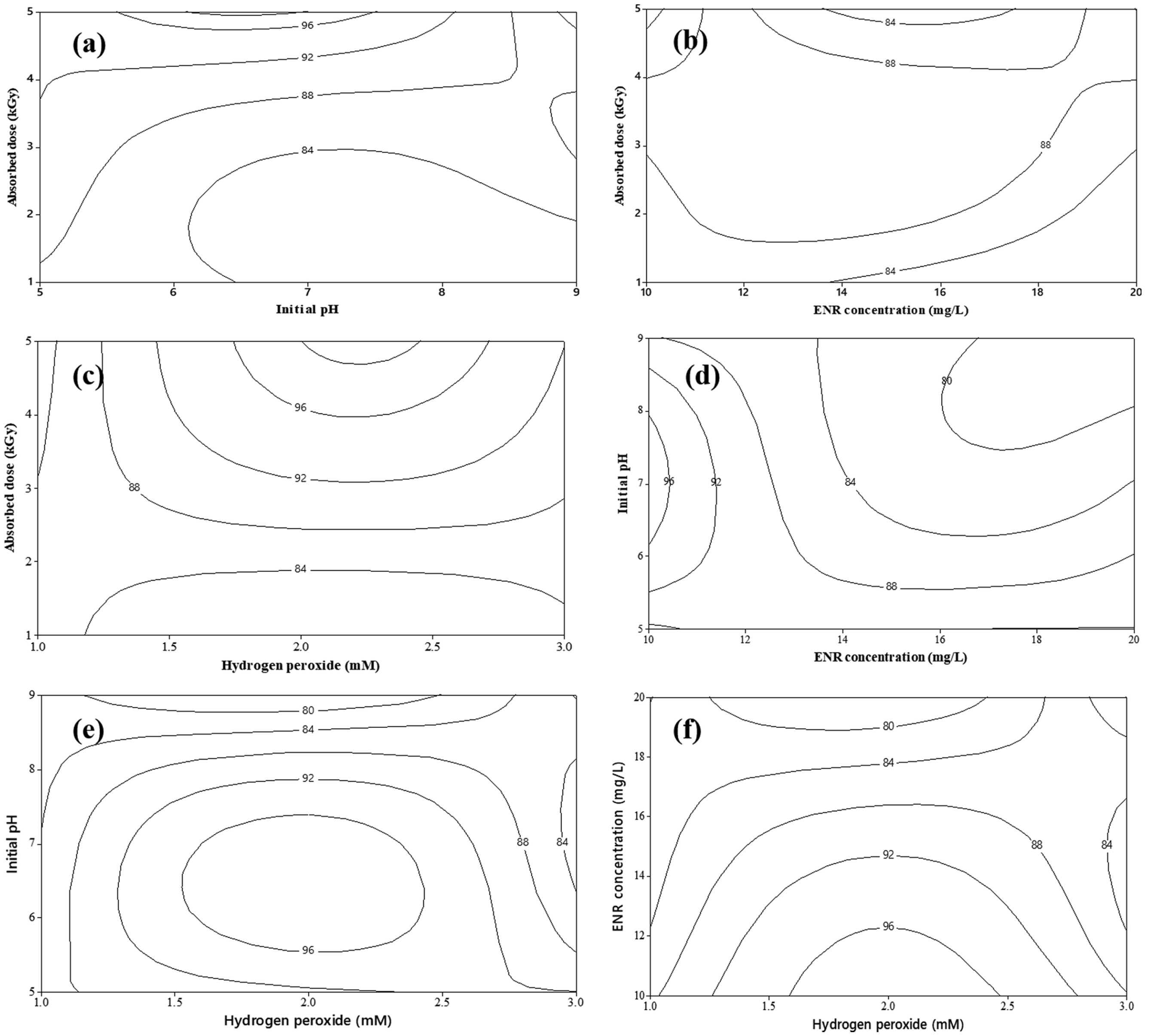

Fig. 6. Contour plot effect of absorbed dose and (a) initial pH, (b) ENR concentration, (c) H_2O_2 dosage and effect of (d) initial pH vs. ENR concentration, (e) Initial pH vs. H_2O_2 dosage and (f) H_2O_2 dosage vs ENR concentration.

by-products increases, and these products act as competitors with ENR, which leads to the removal efficiency going down [26].

4-3. Effect of Hydrogen Peroxide Concentration

Previous studies state that the coupled H_2O_2 and can EB could significantly accelerate $^{\bullet}OH$ generation and improve pollutant removal capacity in some types of wastewater [24,25]. Figs. 5(c), (e), and (f) illustrate the effect of the variation in the H_2O_2 concentrations from 1.0 to 3.0 mM with the initial pH, absorbed dose, and ENR concentration constant. The best ENR removal efficiency (higher 96%) could be reached with H_2O_2 dosage in range 1.5 to 2.5 mM; outside of these values the ENR removal efficiency was reduced. The variation of H_2O_2 dosage on treatment capacity during the EB process could appear in our previous EB study. Duy et al. [25] stated that with an adequate H_2O_2 concentration, the EB decomposition could be accelerated due to higher $^{\bullet}OH$ formation, which is called synergistic effect as following Eqs. (10) and (11). However, the excess H_2O_2 dosage leads to a dominant weaker oxidant (compared to $^{\bullet}OH$) as per Eqs. (14) and (15), the removal capacity decreases.

$$H_2O_2 + {}^{\bullet}OH \rightarrow HO_2^{\bullet} + H_2O \tag{14}$$

$$HO_2^{\bullet} + {}^{\bullet}OH \rightarrow H_2O + O_2 \tag{15}$$

These results are in accord with recent studies indicating that high H_2O_2 dosage could have a negative effect on removal capacity during EB treatment [24,28].

4-4. ENR Degradation Pathways Proposed by Theoretical Approaches

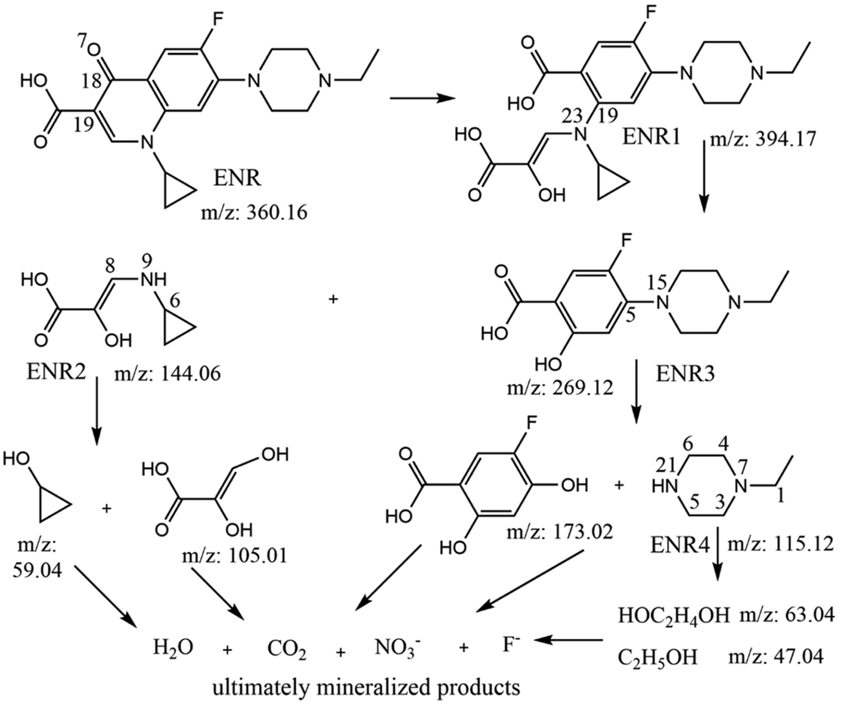

Fig. 7. The highest occurrence of degradation pathways of ENR proposed by theoretical calculations.

As discussed previously (Eqs. (10)-(12)), EB irradiation into an aqueous solution produces strong oxidizing agents, especially when small amounts of hydrogen peroxide are added. These oxidizing agents cause the decomposition of organic pollutants present in aqueous solutions. Because EB has high energy, this irradiation can completely oxidize the pollutant to produce basic inorganic minerals. Pollutant decomposition occurs by an extremely complex mechanism, including many parallel and series reactions if the energy of EB is high. In this section, we explain the degradation pathways of ENR under moderate reaction conditions with the highest occurrence probability based on localized NBO orbital energies. The highest occupied NBO orbital of the ENR molecule is the site of the attack by oxidizing agents with the highest probability in terms of energy [25]. To identify these localized highest occupied NBOs, we optimized the geometric and electronic structures of the ENR and its intermediate products using density functional theory (DFT) based calculations and followed by NBO calculations.

The highest NBO of the ENR molecule is located at the O7 (Fig. 7, Table S3) position, so this position will have the highest probability of being attacked by an oxidizing agent. A peroxide product HOO- can be generated from the O7 site facilitating C18-C19 cleavage due to its high polarity. The carbon atoms C18 and C19 are further oxidized, leading to the attachment of -OH groups and these positions. The intermediate product ENR1 is the result of an oxidant attack on the O7 site. The most active site of the ENR1 molecule is at the N23 atom (lone-pair, −7.12 eV). Of the three single bonds of N23 with three surrounding carbons, the N23-C19 bond has the highest polarization based on the NBO charge distribution. Therefore, under the attack of an oxidizing agent, the N23-C19 bond will be broken, leading to the formation of two intermediates ENR2 and ENR3. The N9 atom is the site with the highest NBO of the ENR2 molecule (−7.37 eV). The N9-C8 and N9-C6 bonds of the ENR2 molecule will be broken, respectively, causing the formation of the next two intermediates, as shown in Fig. 7. The highest lone-pair NBO at position N15 of the ENR3 molecule is the most active site of this molecule. Besides, the N15-C5 bond has the highest polarity of the three bonds of carbon atoms with N15. So, the N15-C5 bond will preferentially be broken to give the intermediate ENR4 and another intermediate with m/z of 172.02. For the ENR4 molecule, the two highest NBOs are located at positions N7 and N21. The breaking of the bonds of the carbon atoms with these two nitrogen atoms will occur in turn in the same way as above. The products of this breakdown can be ethylene glycol and ethanol. However, intermediates containing -OH groups can be oxidized to -C=O or -COOH groups during the reaction. In addition, if EB irradiation is maintained for a long time, it will lead to complete mineralization of the intermediates. Most intermediaries appear on treated spectral MS/MS (Figs. S1 and S2), such as m/z of 269, 173, 144, 115, etc. These results are consistent with the by-products of ENR by photodegradation stated by Babić et al. [17].

5. LCA Results

The parametric life cycle results represent the LCIA metrics for the removal of 1 m^3 of ENR from an aqueous solution using EB irradiation. 22 impact categories on midpoint (GWF, GWT, GWH, OT, OH, SOD, ION, FMF, TA, FE, ME, TE, FE, ME, HCT, HNCT, LU, MRS, FRS, WHH, WTE, and WAE) and three impact items on the endpoint (resource, ecosystems and human health) are used to evaluate ENR treatment. The calculation of the endpoint was estimated EB treatment cost of approximately 0.838 \$/m^3 (E_{con}~ 0.181 \$ and H_2O_2 cost~0.658 \$) computed from Eqs. (8) and (9) at optimal values of $C_{M_{H_2O_2}}$=2 mM and absorbed dose of 5 kGy.

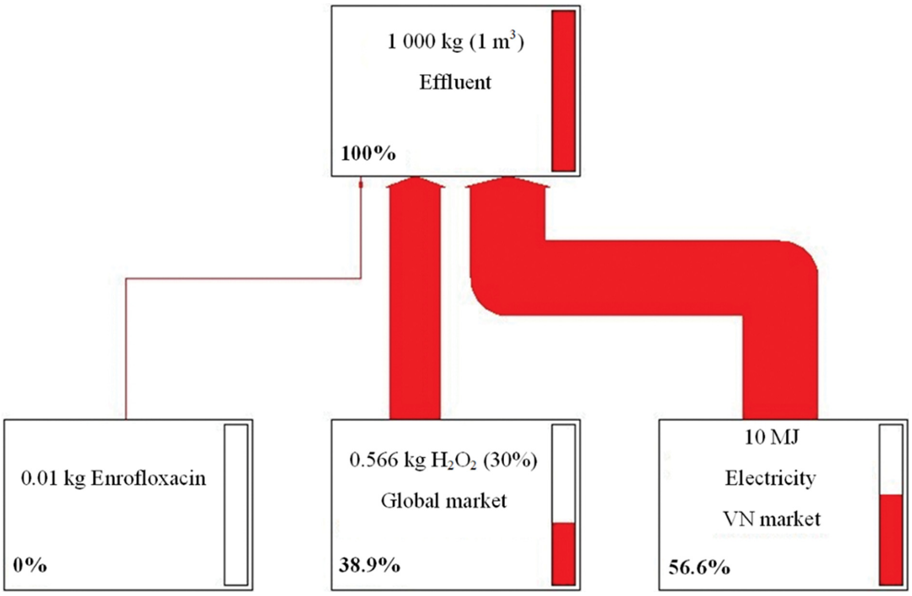

Fig. 8. Dendrogram of input materials and their contributions to environmental impacts for 1 m^3 ENR removal.

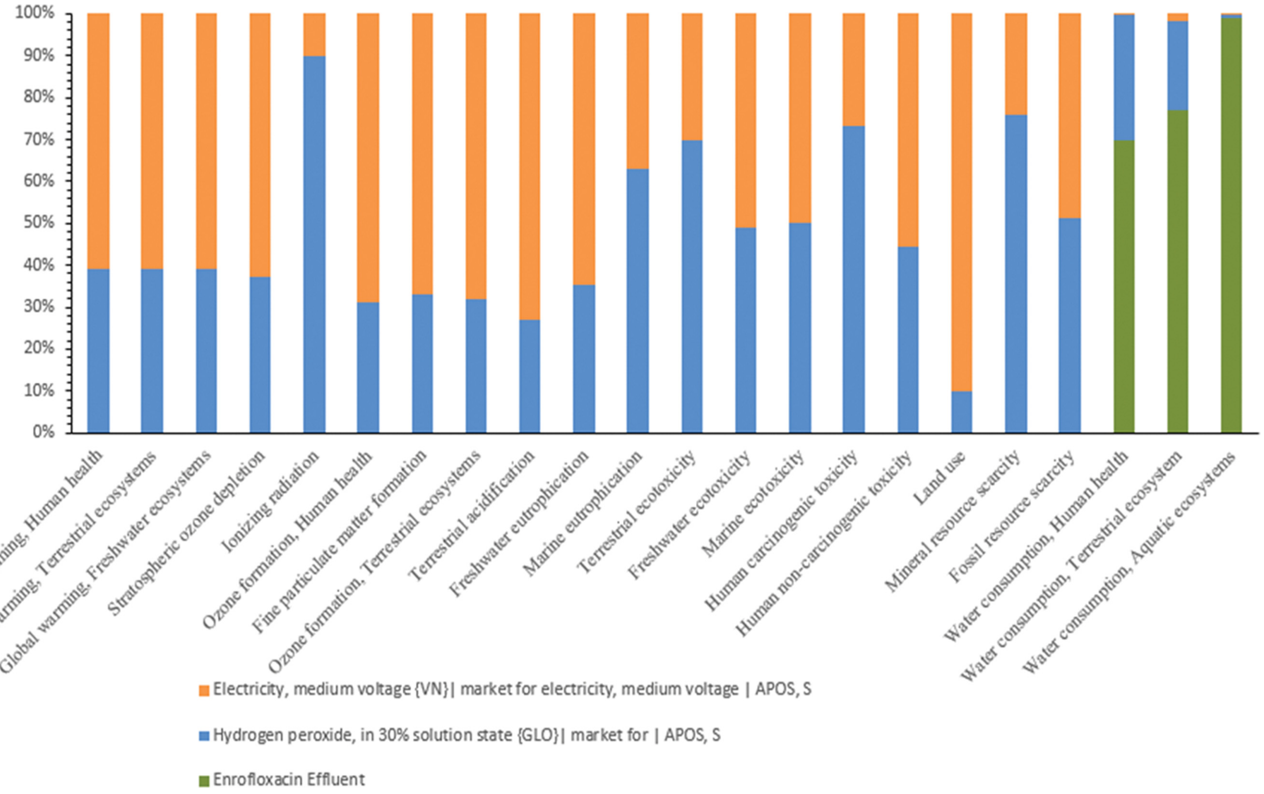

Fig. 9. The contribution of each activity to the environmental impact indicators midpoint.

The LCIA result (Fig. 8) proves that the major contribution for the ENR treatment capacity (10 kg/m^3) is energy (56.6%) followed by H_2O_2 (38.9%), while ENR is negligible on the environmental impacts.

The dominant impact of energy than the impacts of H_2O_2 and ENR is demonstrated in Fig. 9. As seen in the figure, energy significantly influences LU, HNCT, TA, GWF, GWT, GWH, SOD, OH, OT, and FMF while H_2O_2 substantial impact on FRS, MRS, HCT, TE, ME, and ION; and ENR only affects WHH, WTE, WAE, and FE.

Fig. 10 describes the end effects indicators, indicating that energy consumption and H_2O_2 account for over 80%. Based on that, the resource consumption can be ignored if the amount of H_2O_2 is not used to increase the reaction efficiency (about 25%). Still, it

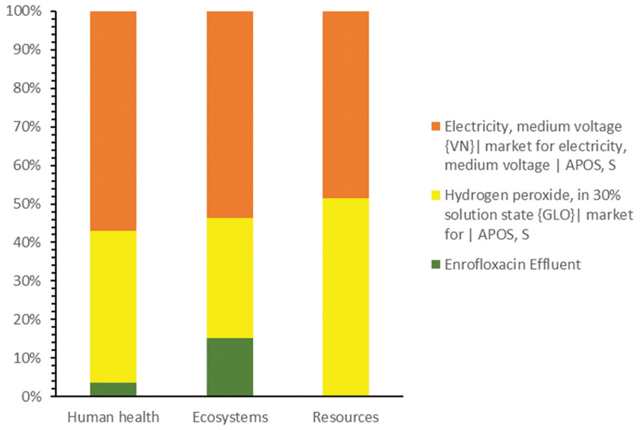

Fig. 10. The contribution of each activity to the environmental impact indicators endpoint.

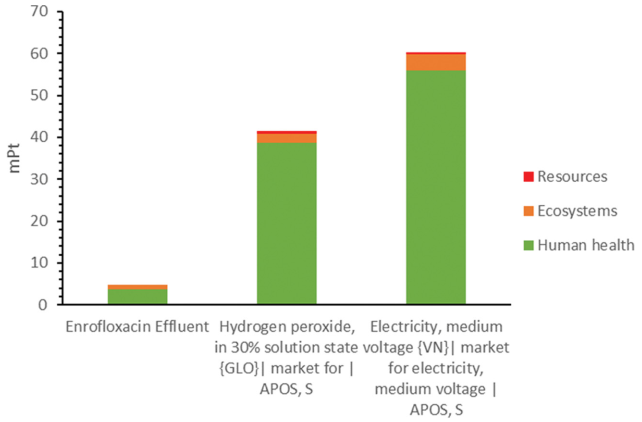

Fig. 12. Endpoint environmental impact categories for removing 10 mg/L ENR by EB process according to the ReCiPe methodology.

affects the ecological and human health indicators due to the amount of ENR discharging effluent into the environment (even with minor concentrations). Therefore, it is possible to balance efficiency and the number of H_2O_2 added impacts are minimal on the environment.

The whole process from midpoint to endpoint could be elucidated on three impacts of human health, ecosystems, and resource, which are displayed in Figs. 11 and 12.

As described in Fig. 11, the three most influential factors are FM, GWH, and HNCT, with the scores as 40.44 mPt, 34.43 mPt, and 10.38 mPt, respectively. It is noticed that these indicators are affected by secondary emissions during chemical and electricity production in Vietnam. Electricity in Vietnam is mainly provided by fossil, water, and natural gas. These compounds contribute to many toxic and hazardous by-products released into the environment, increasing toxicity to humans.

Fig. 12 shows that electricity and H_2O_2 have the most influence on environmental impact with 60.4 mPt and 41.5 mPt contributions, respectively. Human health was most influenced by 98.2, while ecosystems reached 7.33 mPt, and resources seem to be insignificantly affected with 1.1 mPt. It is necessary to use clean energy sources to power the EB systems. These results are consistent with Lee et al.'s [49] finding, which stated that electricity had the greatest effect on environmental impact during the EB process for disinfection.

CONCLUSIONS AND FUTURE PERSPECTIVES

The electron beam process coupled with H_2O_2 was employed to

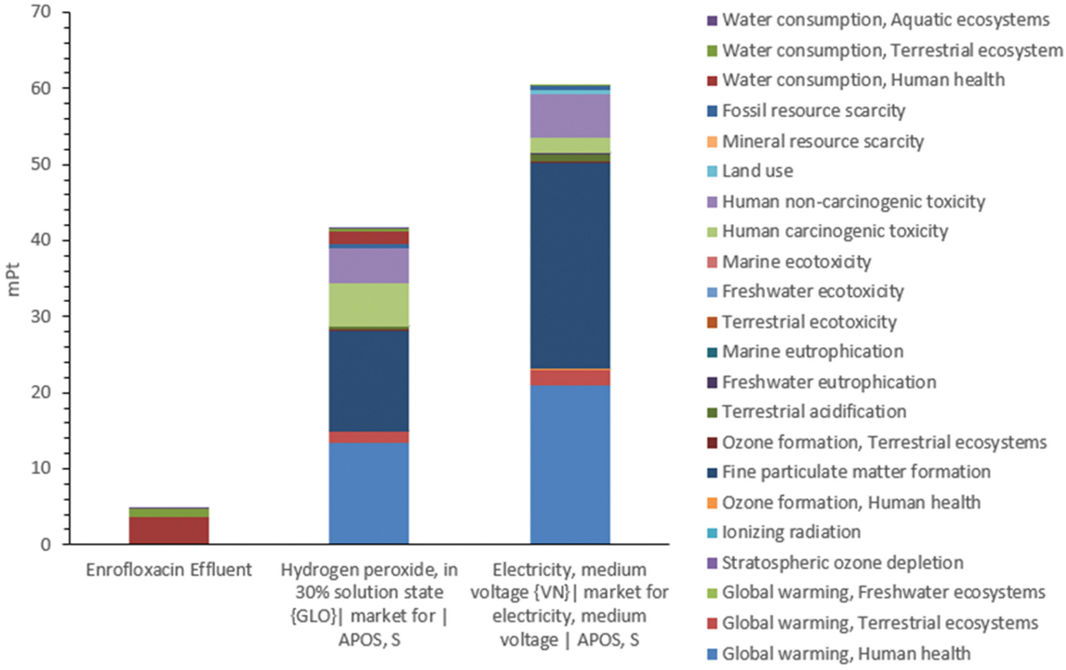

Fig. 11. Environmental impact score for the removal of 10 mg/L ENR by EB process according to the ReCiPe methodology.

treat enrofloxacin (ENR) in an aqueous. In addition, the acute toxicity of this contaminant was evaluated and revealed that ENR exhibits low toxicity against cyanobacterium *Arthrospira* sp. The treatment experiments were conducted at different ENR concentrations, absorbed doses, H_2O_2 dosages, and initial pH values using the Taguchi approach. At optimum values of variables (absorbed dose of 5 kGy, ENR of 10 mg/L, pH of 5, and H_2O_2 concentration of 2 mM), almost all of the ENR was eliminated (98.53%) with a treatment cost of 0.838 $\$/m^3$. The degradation of ENR by EB apparently followed pseudo-first-order kinetics, with R^2 and D_{50} of ~0.9702 and 0.879 kGy, respectively. The major degradation pathways of ENR under EB irradiation were elucidated by DFT theoretical calculations, including NBO analysis. LCA demonstrated that EB's ENR removal is substantially influenced by energy consumption and the amount of H_2O_2. The ReCiPe tool also indicates the consumption and H_2O_2 major affected human health (98.2 mPt), ecosystems (7.33 mPt), and resource consumption (1.1 mPt). The LCA implies that the energy consumption should be optimized and H_2O_2 reduced or replaced with other greener chemicals to decrease the treatment process's harmful effects. Even though these findings revealed that EB radiation demonstrates promise for the degradation of organic pollutants in aqueous solutions, greater efforts are needed to develop the pilot scale for the EB treatment process, which makes the EB more practical application in wastewater treatment fields.

DECLARATIONS

Funding

This work is supported by the Vietnam National Foundation for Science and Technology Development (NAFOSTED) under Grant No. 16/2020/STS02 and Saigon Univesity (TĐ2020-26).

Conflict of Interest

The authors declare that they have no conflict of interest.

Availability of Data and Materials

The data that support the findings of this study are openly available at [DOI].

Code availability (software application or custom code): This study used SimaPro Faculty license with code "FFL Saigon 01".

Author Contributions

The investigation, software, writing - original draft, writing - review & editing: Hong Thi Bich Truong Investigation, software, writing - original draft: Hiep Nghia Bui; Data curation, conceptualization, methodology: Hieu Trung Nguyen and Thanh-Luu Pham; Investigation, software, writing - original draft: Van-Truc Nguyen, Duy Ngoc Nguyen, Thi-Dieu-Hien Vo and Yuan-Shing Perng; Funding acquisition, supervision, conceived, designed the methodology, writing - review & editing: Ha Manh Bui and Linh Thi My Lam.

Consent to Participate

The authors have been personally and actively involved in substantive work leading to the manuscript and will hold themselves jointly and individually responsible for its content.

Consent to Publish

The authors consent to publish this research.

Ethical Approval

The authors confirm that the manuscript has been read and approved by all authors. The authors declare that this manuscript has not been published and not under consideration for publication everywhere.

SUPPORTING INFORMATION

Additional information as noted in the text. This information is available via the Internet at http://www.springer.com/chemistry/journal/11814.

REFERENCES

1. WHO, *Pharmaceuticals in drinking water public health and environment, water, sanitation, hygiene and health*, WHO, Geneva, Switzerland (2011).
2. V. J. Sharavanan, M. Sivaramakrishnan, N. Sivarajasekar, N. Senthilrani, R. Kothandan, N. Dhakal, S. Sivamani, P. L. Show, M. R. Awual and M. Naushad, *Environ. Chem. Lett.*, **18**, 325 (2020).
3. E. Mohmmed, A. M. Abdelkarim, M. A. Oshi and M. Naeem, *Life Sci.*, **2**, 4 (2021).
4. I. Ebert, J. Bachmann, U. Kühnen, A. Küster, C. Kussatz, D. Maletzki and C. Schlüter, *Environ. Toxicol. Chem.*, **30**, 2786 (2011).
5. R. Nelson, *Lancet Infect. Dis.*, **4**, 258 (2004).
6. C. Nguyen Dang Giang, Z. Sebesvari, F. Renaud, I. Rosendahl, Q. Hoang Minh and W. Amelung, *PloS One*, **10**, 0131855 (2015).
7. R. Wei, F. Ge, M. Chen and R. Wang, *J. Environ. Qual.*, **41**, 1481 (2012).
8. M. Andrieu, A. Rico, T. M. Phu, N. T. Phuong and P. J. Van Den Brink, *Chemosphere*, **119**, 407 (2015).
9. G. Li, H. Yang, T. An and Y. Lu, *Ecotoxicol. Environ. Saf.*, **158**, 154 (2018).
10. H. M. Ötker and I. Akmehmet-Balcıoğlu, *J. Hazard. Mater.*, **122**, 251 (2005).
11. G. P. Udayakumar, S. Muthusamy, B. Selvaganesh, N. Sivarajasekar, K. Rambabu, S. Sivamani, N. Sivakumar, J. P. Maran and A. Hosseini-Bandegharaei, *Biotechnol. Adv.*, **52**, 107815 (2021).
12. S. Muthusaravanan, K. Balasubramani, R. Suresh, R. S. Ganesh, N. Sivarajasekar, H. Arul, K. Rambabu, G. Bharath, V. E. Sathishkumar, A. P. Murthy and F. Banat, *Environ. Res.*, **200**, 111428 (2021).
13. K. Balasubramani, N. Sivarajasekar and M. Naushad, *J. Mol. Liq.*, **301**, 112426 (2020).
14. D. Li, J. Gao, H. Dai, Z. Wang and W. Duan, *Bioresour. Technol.*, **312**, 123567 (2020).
15. M. B. Ahmed, J. L. Zhou, H. H. Ngo and W. Guo, *Sci. Total Environ.*, **532**, 112 (2015).
16. Z. Lu, F. Chen, M. He, M. Song, Z. Ma, W. Shi, Y. Yan, J. Lan, F. Li and P. Xiao, *Chem. Eng.*, **249**, 15 (2014).
17. S. Babić, M. Periša and I. Škorić, *Chemosphere*, **91**, 1635 (2013).
18. K. Balasubramani, N. Sivarajasekar, S. Muthusaravanan, K. Ram, M. Naushad, T. Ahamad and G. Sharma, *J. Mol. Liq.*, **319**, 114371 (2020).
19. M.-S. Han, Y.-W. Choi, J.-H. Song and C.-K. Wang, *J. Korean Soc. Water Environ.*, **34**, 149 (2018).
20. M. Kermani, F. Bahrami Asl, M. Farzadkia, A. Esrafili, S. Salahshour Arian, M. Khazaei, Y. Dadban Shahamat and D. Zeynalzadeh, *Desalin. Water Treat.*, **57**, 16435 (2016).

21. H. Guo, N. Gao, Y. Yang and Y. Zhang, *Chem. Eng.*, **292**, 82 (2016).
22. Y. D. Shahamat, M. A. Zazouli, M. R. Zare and N. Mengelizadeh, *Rsc Adv.*, **9**, 16496 (2019).
23. X. Li, C. Xiao, X. Ruan, Y. Hu, C. Zhang, J. Cheng and Y. Chen, *Chem. Eng.*, **427**, 130927 (2022).
24. N. N. Duy, T. N. Hieu, T. P. Luu, X. B. Thanh, T. D. Thuy, J. J. Jiang, Y. S. Perng, F. Boujelbane and M. B. Ha, *J. Water Process. Eng.*, **40**, 101781 (2021).
25. N. N. Duy, T. N. Hieu, T. P. Luu, T. N. Cong, T. G. D. Huong, Q. N. Hien, Y. C. Chen, N. B. Hiep, T. D. V. Hien, V. N. Truc and M. B. Ha, *Environ. Technol. Innov.*, **21**, 101315 (2021).
26. L. Jia-Tong, L. Yong-Sheng, S. Qing, H. Da-Qian, Z. Dan and J. Wen-Bao, *J. Adv. Oxid. Technol.*, **20**, 20160173 (2017).
27. F. K. Tominaga, A. P. Dos Santos Batista, A. C. S. C. Teixeira and S. I. Borrely, *J. Environ. Chem. Eng.*, **6**, 4605 (2018).
28. C. N. Kurucz, T. D. Waite and W. J. Cooper, *Radiat. Phys. Chem.*, **45**, 299 (1995).
29. N. N. Duy, D. Van Phu, N. T. K. Lan, N. T. Duoc, N. Q. Hien, B. N. Hiep, B. N. Han and B. M. Ha, *Acta Chem. Iasi*, **27**, 303 (2019).
30. T. H. Kim, Y. K. Nam and M. J. Lee, *J. Korean Phys. Soc.*, **54**, 2109 (2009).
31. J.-Y. Cho, *Bull. Environ. Contam. Toxicol.*, **84**, 450 (2010).
32. W. Han, C. Zhong, L. Liang, Y. Sun, Y. Guan, L. Wang, X. Sun and J. Li, *Electrochim. Acta*, **130**, 179 (2014).
33. P. Nazari and S. R. Setayesh, *Int. J. Environ. Sci. Technol.*, **16**, 6329 (2019).
34. R. Changotra, J. P. Guin, S. A. Khader, L. Varshney and A. Dhir, *Chem. Eng.*, **356**, 973 (2019).
35. F. Özyonar, *Cumhuriyet Sci. J.*, **39**, 1127 (2018).
36. M. H. Rasoulifard, M. Akrami and M. R. Eskandarian, *J. Taiwan Inst. Chem. Eng.*, **57**, 77 (2015).
37. Ö. Gökkuş, N. Yıldız, A. S. Koparal and Y. Yıldız, *Int. J. Environ. Sci. Technol.*, **15**, 449 (2018).
38. M. Gholami, B. A. Souraki, A. Pendashteh, S. P. Mozhdehi and M. B. Marzouni, *Desalin. Water Treat.*, **95**, 96 (2017).
39. J. Kotai, *Instructions for preparation of modified nutrient solution Z8 for algae*, Norwegian Institute for Water Research Publications, Oslo (1972).
40. OECD, *Guidelines for testing of chemicals: Freshwater alga and cyanobacteria, growth inhibition test*, Organization for the Economical Cooperation and Development, Paris, France (2006).
41. ASTM, ISO/ASTM, 51275-13 (2004).
42. A. A. Elezz, A. Easa, F. Atia and T. Ahmed, *Data Br.*, **25**, 104326 (2019).
43. W. Klöpffer, *Int. J. Life Cycle Assess*, **17**, 1087 (2012).
44. B. V. Pré Sustainability, Simapro (2021).
45. E. Chatzisymeon, S. Foteinis, D. Mantzavinos and T. Tsoutsos, *J. Clean. Prod.*, **54**, 229 (2013).
46. H. Qin, L. Chen, N. Lu, Y. Zhao and X. Yuan, *Front. Environ. Sci. Eng.*, **6**, 107 (2012).
47. J.-Q. Xiong, M. B. Kurade and B.-H. Jeon, *Environ. Pollut.*, **226**, 486 (2017).
48. P. T. T. Nguyen, H. T. Nguyen, U. N. P. Tran and H. Manh Bui, *J. Chem.*, **9981738**, 1 (2021).
49. K.-M. Lee, S. Yu, Y.-H. Choi and M. Lee, *Int. J. Life Cycle Assess*, **17**, 565 (2012).

Supporting Information

A Taguchi approach with electron-beam irradiation to optimize the efficiency of removing enrofloxacin from aqueous media

Hong Thi Bich Truong*, **Hiep Nghia Bui****, **Hieu Trung Nguyen*****, **Thanh-Luu Pham******,*****,
Duy Ngoc Nguyen******, **Yuan-Shing Perng*********, **Linh Thi My Lam**********,*********,
Thi-Dieu-Hien Vo**********, **Van-Truc Nguyen*************, **and Ha Manh Bui*************,†

*Department of Chemistry, Biology and Environment, Pham Van Dong University, Quang Ngai Province 57000, Vietnam
**Department of Environmental Engineering, Dayeh University, Changhua 51591, Taiwan
***Institute of Applied Technology, Thu Dau Mot University, Thu Dau Mot City, Binh Duong Province 75000, Vietnam
****Graduate University of Science and Technology, Vietnam Academy of Science and Technology, Hanoi 10000, Viet Nam
*****Institute of Tropical Biology, Ho Chi Minh City 70000, Vietnam
******Research and Development Center for Radiation Technology, Vietnam Atomic Energy Institute,
Ho Chi Minh City 70000, Vietnam
*******Department of Forestry, National Chung Hsing University, Taichung 40227, Taiwan
********Faculty of Education, An Giang University, An Giang Province 90000, Vietnam
*********Vietnam National University Ho Chi Minh City, Ho Chi Minh City 70000, Vietnam
**********Faculty of Environmental and Food Engineering, Nguyen Tat Thanh University,
Ho Chi Minh City 70000, Vietnam
***********Department of Environmental Sciences, Saigon University, Ho Chi Minh City 70000, Vietnam

(*Received 18 August 2021 • Revised 12 October 2021 • Accepted 24 October 2021*)

Table S1. Response for the signal to noise ratios

Level	Initial pH	ENR con. (mg/L)	H_2O_2 dosage (mM)	Absorbed dose (kGy)
1	39.10	39.19	38.54	38.26
2	38.89	38.61	38.89	38.88
3	38.29	38.48	38.85	39.13
Delta	0.82	0.71	0.36	0.87
Rank	2	3	4	1

Table S2. Response for means

Level	Initial pH	ENR con. (mg/L)	H_2O_2 dosage (mM)	Absorbed dose (kGy)
1	90.22	91.18	84.52	82.02
2	88.27	85.36	88.52	87.96
3	82.24	84.19	87.68	90.75
Delta	7.98	6.99	4.00	8.73
Rank	2	3	4	1

Table S3. The highest occupied NBOs of ENR and its intermediates

No.	Molecule	Highest occupied NBO orbital	NBO type	Energy (eV)
1	ENR	O7	Lone-pair	−7.02
2	ENR1	N23	Lone-pair	−7.12
3	ENR2	N9	Lone-pair	−7.37
4	ENR3	N15	Lone-pair	−7.16
5	EBR4	N7	Lone-pair	−7.58

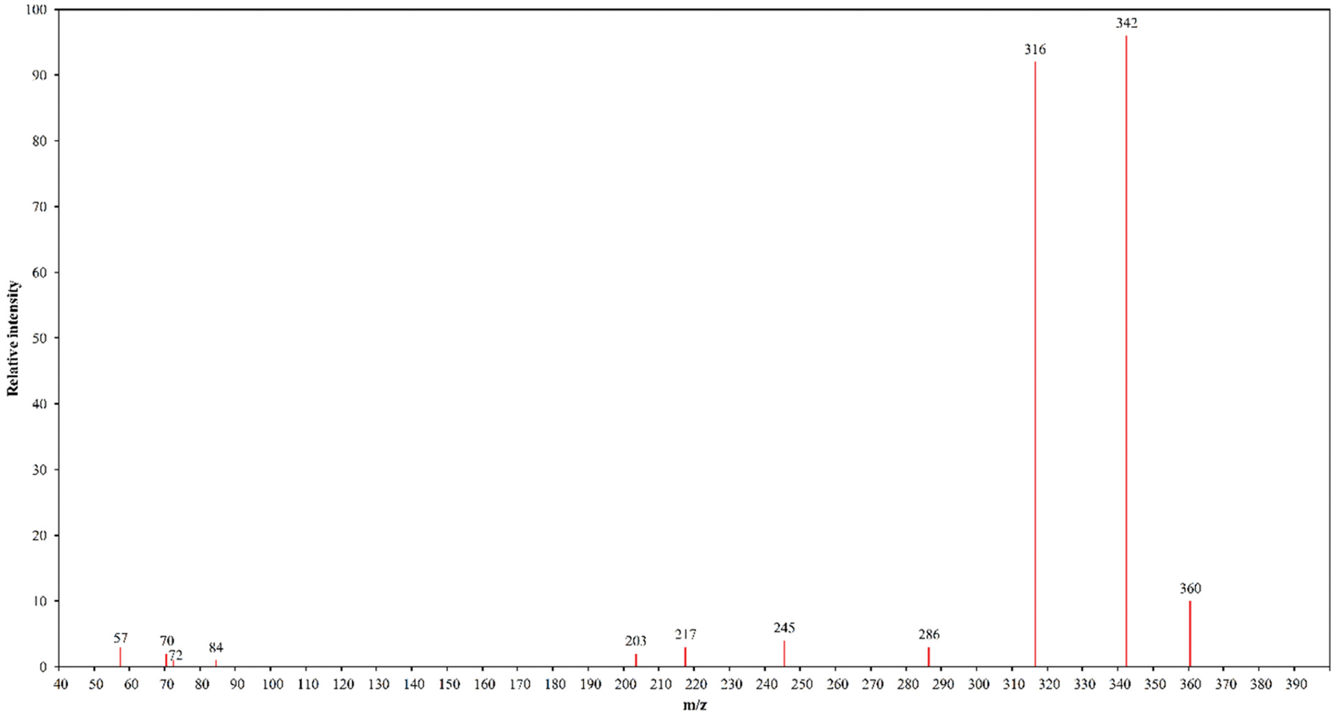

Fig. S1. Mass spectra of the original ENR solutions.

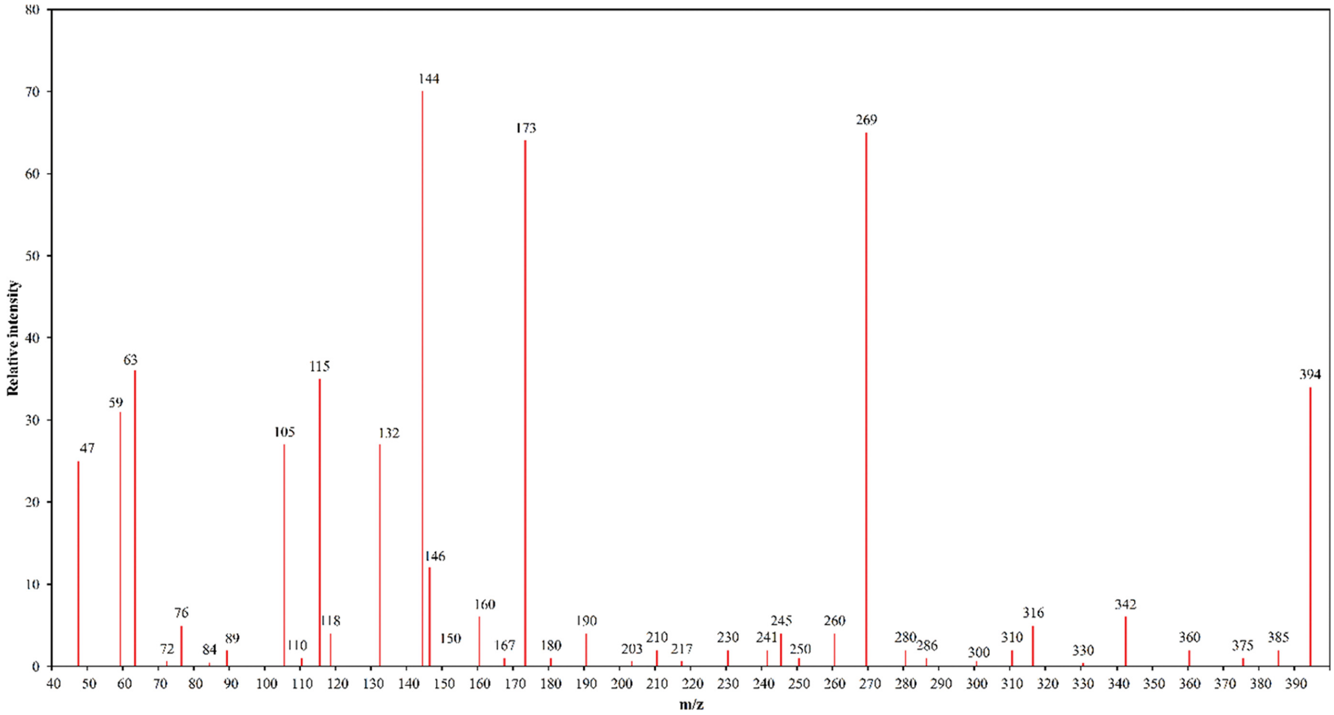

Fig. S2. Mass spectra of the original ENR solutions obtained after EB treatment.